

Thesis title: Investigation on the non-trivial dielectric, piezoelectric and vibrational properties of some lead-free multifunctional nanomaterials

Index No. – 130/19/Phys./26

Registration No. – SOPHY1113019

Abstract

Recently, the pursuit of lead-free, non-toxic, and environment-friendly nanomaterials has emerged as a crucial thrust in scientific research, driven by the increasing awareness of the adverse effects associated with the traditional lead-based counterparts. Factually, many lead-based perovskites and other materials exhibit appreciable ferroelectric, piezoelectric, mechanical and multiferroic properties, that find applications across different energy harvesting/storage-based industries and electrical/electronic gadgets at the cost of severe lead-pollution. This thesis therefore intends to recognise a number of lead-free nanomaterials, which are fundamentally appealing as well as technologically sound (such as iron oxides: magnetite, hematite and maghemite; polymeric nanocomposites; perovskite titanates; rare-earth sesquioxides; *etc.*), and to investigate particular electrical, optical and vibrational properties with an aim of multifunctional applications. The first three chapters of this thesis are dedicated for introductory concepts, realizing the research motivation, a thorough review of the background theories and literature, and the details of the instrumental and computational facilities available for our projects, respectively. Thereafter, five of the recently published works are comprehended in the successive chapters (summarised below) with a complete set of associated data, followed by a concluding chapter on the final inferences and future prospects.

Monodispersed and highly water-dispersible, spherical magnetite (Fe_3O_4) nanoparticles with a size range of 3.7 – 242.8 nm has been synthesized using a microwave-assisted solvothermal approach, that features excellent colloidal stability due to surface functionalization. The variation in optical bandgap from 1.59 to 4.92 eV with size contraction has been explained with crystal field theory and quantum confinement effects. The Raman peaks also exhibit a red-shift and gradually developed Fano asymmetry in the line-shape as indicated by the phonon confinement model. Mössbauer analysis evidenced the transition from ferrimagnetic to superparamagnetic nature with reduction in particle size. These stoichiometric, non-toxic, and magnetic nanocrystals have potential applications in biomedicine as well as electroactive porous host networks. When incorporated into poly(vinylidene fluoride)-based nanogenerators, excellent piezoelectric performance in terms of open circuit voltage, short circuit current and as-delivered power (can glow long series of LEDs) is achieved, along with substantial electromagnetic interference shielding capabilities.

Moreover, persistent low-frequency negative capacitance (NC) dispersion has been detected in polycrystalline Fe_3O_4 nanoparticles of varying sizes under moderate DC bias. The relaxation times, shape parameters, and resistivity of the nanoparticles are analysed using the Havriliak-Negami model and 3D Cole-Cole plots. The universal Debye relaxation theory is modified to account for the shifted quasi-static NC dispersion plane in materials exhibiting both positive and negative capacitances around a transition frequency (f_0), which was found to blue-shift with increasing external field and decreasing particle size. A generalized dispersion scheme is proposed to fit both positive and negative capacitance regimes, including the transition point. A comprehensive model using phasor diagrams is discussed to differentiate various NC mechanisms. The presence of iron vacancies in the nanoparticles, validated by first principles calculations, is suggested as the contributor in their p-type nature and the stabilization of NC.

An analytical impedance and dielectric analysis are conducted on two cardinal ferric oxide polymorphs *viz.*, hematite (α – Fe_2O_3) and maghemite (γ – Fe_2O_3) nanoparticles. Non-Debye dipolar relaxations, small polaron hopping conduction, and resistivity correlations are quantified, along with the delocalization and de-trapping of carriers under a DC field. The dielectric constant is enhanced at low frequencies by Maxwell-

Wagner polarization, addressing energy storage solutions. Thereafter, the optical dielectric function and associated parameters are evaluated using a density functional theory (DFT) + U framework, considering resonant absorption, dissipation, electronic polarization, and decay. A vacancy-ordered maghemite-type supercell is constructed for efficient computational cost. Finally, the anisotropy in materials sensitive to photonic excitations is examined through simulations of the energy-dispersive evolution of the dielectric ellipsoid to advance the understanding of linear and nonlinear dielectrics in materials physics.

The impact of DC field is further investigated on the impedance, dielectric, admittance, and modulus spectra of polycrystalline calcium, strontium, and barium titanate nanoparticles. After elementary characterizations to validate the phase conformation, stoichiometry, optical, and vibrational attributes, the effects of the external field on the real and imaginary parts of impedance, dielectric functions, and related properties are studied for energy storage applications. Electrically heterogeneous grain core-grain boundary (GC-GB) resistance correlations are quantified using proposed equivalent circuitry and Nyquist plots. The relaxation times, shape parameters, and frequency limits are determined using Cole-Davidson and Johnson's equations, elucidating Maxwell-Wagner interfacial polarization. Non-Debye relaxations are analysed using the modified Kohlrausch-Williams-Watts (KWW) equation, highlighting asymmetric broadening in modulus spectra. Large polaron hopping conduction is investigated using Jonscher's power law, considering variable-range and correlated barrier hopping mechanisms. DFT is utilized to understand static dielectric tensors, Born effective charges, and field-induced charge cloud separation. Finite element simulations using experimentally derived electrical parameters, validate non-uniform and anisotropic field-diffusion within the GC-GB heterostructure.

Laser power-dependent Raman spectroscopy is used to investigate Fano interference between the electronic continuum and discrete phonon modes for selected rare-earth sesquioxide systems. The Raman-active optic modes in different phases are analysed through group theoretical analysis, and laser heating-induced local phase transitions are identified. Increasing laser intensity leads to a redshift and larger negative asymmetry in the Raman peaks, attributed to modifications in Fano scattering and enhanced electron-phonon coupling amid the photoexcited electron plasma. Empowered by the high sensitivity of spectral peaks to excitation strength, the intrinsic nature of the discrete-continuum Fano resonance in the nanoparticles is quantitatively studied in terms of the interference conditions, force constant, bond lengths, tensile stress, *etc.* and as a function of lattice temperature. The charge-phonon coupling constant (λ) increases with laser power, indicating stronger particle-quasiparticle coupling, while a shorter anharmonic phonon lifetime (τ_{anh}) suggests faster interactions. Using Allen's formalism, the charge density of states ($N(\epsilon_F)$) at the Fermi level is calculated, showing a negative regression dependence in the dynamics of $\lambda N(\epsilon_F)$ and τ_{anh} .


Keywords: Dielectric properties, Impedance spectroscopy, Piezoelectric nanogenerator, Negative capacitance, Lead-free nanomaterials, PVDF nanocomposites, Fe_3O_4 , Ferric oxide, Perovskite titanate, Rare-earth sesquioxide, Raman spectroscopy, Fano interference.

Souvik Bhattacharjee.

Signature of the candidate

(Souvik Bhattacharjee)

Date: 28/06/2023.



Signature of the supervisor

(Prof. Kalyan Kumar Chattopadhyay)

Date: 28.06.23

Dr. K. K. Chattopadhyay
Professor
Head, Department of Physics
Jadavpur University
Kolkata-700 032